The focal length was optimized at each scan angle by judging the quality of the radiation pattern. The optimum feed position loci were found to be linear as shown in Fig. 1. By plotting all values of β (beam scan angle) for each 2.5° change in β' (feed scan angle), it was found that the beam deviation factor was essentially linear with $\beta = 1.076\beta'$. This factor is slightly greater than unity in contrast to a conventional parabolic antenna whose beam deviation factor is less than unity.

The gain and efficiency characteristics as a function of scan angle are shown in Fig. 5. For a 3-dB drop in gain, the beam may be steered to 18° or 7.65 beamwidths. The half-power beamwidth and the first sidelobe level as a function of scan angle, both in the plane of scan and perpendicular to the plane of scan, are also shown in this figure. For the 18° scan, the sidelobe level has increased to −11 dB from the on-axis value of −22.5 dB. The measured VSWR as a function of scan angle remained essentially constant.

IV. Conclusions

Some of the significant electrical characteristics of a 3-foot-diameter circularly polarized metallic lens antenna have been established. On the basis of this limited study, a few observations may be made. The efficiency of this lens is somewhat lower than that of conventional reflector antennas. The lens was designed for an index of refraction equal to 0.5, which requires operating the waveguide medium fairly close to cutoff. If a lens were designed with a higher index of refraction, the total number of waveguides required for a given diameter would be reduced and the effects of dispersion minimized. The bandwidth of this lens is limited by its thickness; zoning or reducing the thickness would improve the bandwidth.

H. E. King
J. L. Wong
R. B. Dybdal
M. E. Schwartz
Aerospace Corp.
El Segundo, Calif.

References

[1] W. E. Kock, "Metal-lens antenna," *Proc. IRE*, vol. 34, pp. 828–836, November 1946.
[2] S. Silver, *Microwave Antenna Theory and Design*. New York: McGraw-Hill, 1949, pp. 402–412.
[3] F. E. Cook and E. M. Polzin, "A hardened ground antenna design concept for space communications," Aerospace Corp., El Segundo, Calif., Rept. TOR-0066(5413)-1, July 1, 1969.
[4] H. E. King, J. L. Wong, R. B. Dybdal, and M. E. Schwartz, "Electrical characteristics of a hardenable, circularly polarized metallic lens antenna," Aerospace Corp., El Segundo, Calif., Rept TR-0066 (5320)-4, January 30, 1970.
[5] M. Born and E. Wolf, *Principles of Optics*. New York: Pergamon, 1964, p. 163.
[6] J. R. Pyle, "Circular polarizers of fixed bandwidth," *IEEE Trans. Microwave Theory and Techniques* (Correspondence), vol. MTT-12, pp. 557–559, September 1964.

Mutual Impedance Between Coplanar-Skew Dipoles

***Abstract*—The induced EMF formulation is employed to develop a closed-form expression for the mutual impedance between coplanar-skew dipoles. Numerical results are presented in graphical form.**

I Introduction

King [1] has determined the mutual impedance between parallel dipoles, and Lewin [2] has analyzed the coplanar-skew dipoles. Lewin's analysis, however, is restricted to half-wave center-fed dipoles. In this paper we derive an expression for the mutual impedance between coplanar-skew dipoles with arbitrary lengths and terminal positions. This expression is relatively simple and convenient for computer programming.

In Section II we present a new expression for the near-zone field of a linear dipole, in a form most convenient for the mutual-impedance analysis.

Manuscript received October 1, 1969. This work was supported in part by the Department of the Army, Ballistic Research Laboratory, Aberdeen Proving Ground, Md., under Contract DAAD05-69-C-0031 with the Ohio State University Research Foundation.

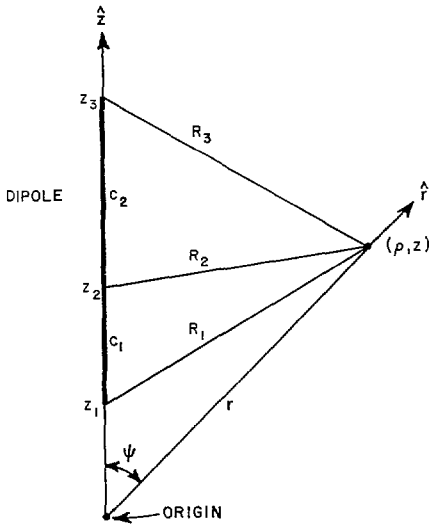

Fig. 1. Linear dipole and coordinate system.

II. The Near-Zone Field of the Linear Dipole

As shown in Fig. 1, we consider a dipole located on the z axis and let z_1 and z_3 denote the endpoints and z_2 the terminals. In the induced EMF method, the dipole current is given by

$$I(z) = \hat{z} I_1 \frac{\sin k(z - z_1)}{\sin kc_1}, \quad z_1 < z < z_2 \tag{1}$$

$$I(z) = \hat{z} I_1 \frac{\sin k(z_3 - z)}{\sin kc_2}, \quad z_2 < z < z_3. \tag{2}$$

The time dependence exp ($j\omega t$) is suppressed, c_1 and c_2 denote the dipole arm lengths, $\hat{z}$ is a unit vector, I_1 is the terminal current, and $k = 2\pi/\lambda$. The field generated in free space by this dipole (or sinusoidal line source) is determined most readily from the expressions of Schelkunoff and Friis [3]. The cylindrical components of the electric field intensity are

$$E_\rho = \frac{j30I_1}{\rho}\left[\frac{(z - z_1)\exp(-jkR_1)}{R_1 \sin kc_1} - \frac{(z - z_2)\exp(-jkR_2)\sin kc}{R_2 \sin kc_1 \sin kc_2} + \frac{(z - z_3)\exp(-jkR_3)}{R_3 \sin kc_2}\right] \tag{3}$$

$$E_z = j30I_1\left[-\frac{\exp(-jkR_1)}{R_1 \sin kc_1} + \frac{\exp(-jkR_2)\sin kc}{R_2 \sin kc_1 \sin kc_2} - \frac{\exp(-jkR_3)}{R_3 \sin kc_2}\right] \tag{4}$$

where c is the dipole length and R_1, R_2, and R_3 are the distances defined in Fig. 1.

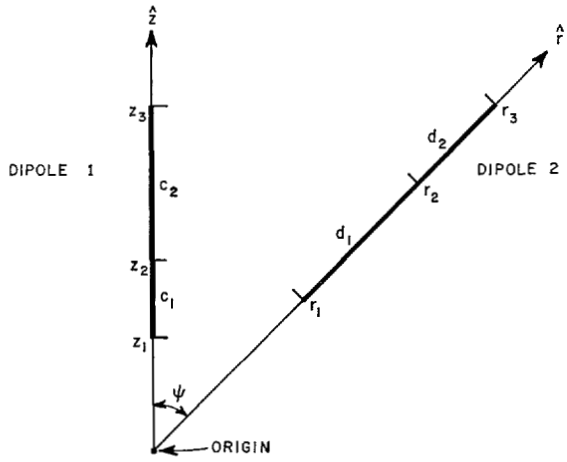

Fig. 2. Coplanar-skew dipoles.

The radial component of the field is obtained from a linear combination of E_ρ and E_z:

$$E_r = \frac{-j30I_1}{r} \sum_{m=1}^{3} C_m z_m \frac{\exp(-jkR_m)}{R_m} \tag{5}$$

where

$$C_1 = 1/(\sin kc_1) \tag{6}$$

$$C_2 = -(\sin kc)/(\sin kc_1 \sin kc_2) \tag{7}$$

$$C_3 = 1/(\sin kc_2). \tag{8}$$

Equation (5) is believed to be a new and useful form for the rigorous near-zone field of the linear dipole.

III. The Mutual Impedance

For the coplanar-skew dipoles shown in Fig. 2, the mutual impedance is

$$Z_{12} = -\frac{1}{I_1 I_2} \int_{r_1}^{r_3} I_2(r) \cdot E_1(r)\, dr. \tag{9}$$

The current on dipole 2 is

$$I_2(r) = \hat{r} \frac{I_2 \sin k(r - r_1)}{\sin kd_1}, \quad r_1 < r < r_2 \tag{10}$$

$$I_2(r) = \hat{r} \frac{I_2 \sin k(r_3 - r)}{\sin kd_2}, \quad r_2 < r < r_3. \tag{11}$$

From (5) and (9),

$$Z_{12} = \frac{j30}{I_2} \sum_{m=1}^{3} z_m C_m \int_{r_1}^{r_3} \frac{I_2(r) \exp(-jkR_m)\, dr}{rR_m}. \tag{12}$$

These integrals are given in terms of the sine and cosine integrals as follows:

$$z_m \int_{r_1}^{r_2} \frac{\exp(\pm jr) \exp(-jR_m)\, dr}{rR_m} = [\exp(-jz_m) E(R_m - z_m \mp r) - \exp(jz_m) E(R_m + z_m \mp r)]_{r_1}^{r_2} \tag{13}$$

where

$$E(x) = Ci(|x|) - jSi(x). \tag{14}$$

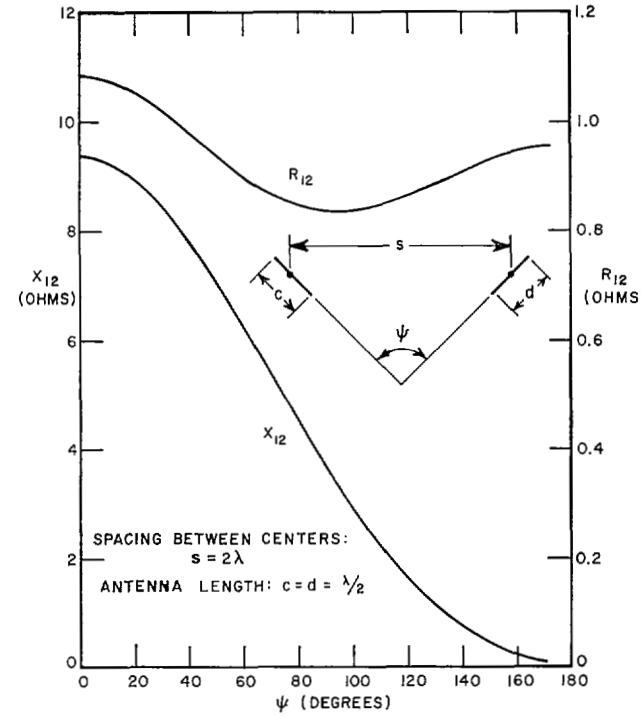

Fig. 3. Mutual impedance between coplanar-skew dipoles.

From (12) and (13), the mutual impedance is

$$Z_{12} = -15 \sum_{m=1}^{3} \sum_{n=1}^{3} C_m D_n \sum_{p=-1}^{1} \sum_{q=-1}^{1} pq \exp[jk(pz_m + qr_n)] \cdot E(kR_{mn} + kpz_m + kqr_n) \tag{15}$$

where p and q assume only the values ± 1, and R_{mn} is the distance from point z_m on dipole 1 to point r_n on dipole 2

$$R_{mn} = (z_m^2 + r_n^2 - 2z_m r_n \cos\psi)^{1/2}. \tag{16}$$

The coefficients D_n have the same form as the C_m

$$D_1 = 1/(\sin kd_1) \tag{17}$$

$$D_2 = -(\sin kd)/(\sin kd_1 \sin kd_2) \tag{18}$$

$$D_3 = 1/(\sin kd_2). \tag{19}$$

The coordinates z_m and r_n are measured from the coordinate origin at the intersection of the axes of the coplanar-skew dipoles. For center-fed half-wave dipoles, (15) reduces to (15) of Lewin's paper [2].

For parallel dipoles, z_m and r_n go to infinity and it is not difficult to show that (15) reduces to the expression published by H. E. King [1].

IV. Numerical Results

Fig. 3 illustrates the mutual impedance between half-wave center-fed dipoles as a function of the angle ψ between their axes. Using (15), the calculations require 0.15 seconds on an IBM 7094 computer for each value of ψ.

Although the numerical approach of Baker and LaGrone [4] is efficient when the dipoles are adequately separated, (15) is preferable for closely spaced dipoles.

V. Conclusion

A convenient new form is presented for the rigorous near-zone field of the linear dipole with sinusoidal current distribution. This is employed to derive a closed-form expression for the mutual impedance between coplanar-skew dipoles.

J. H. Richmond
N. H. Geary
ElectroScience Laboratory
Dept. of Elec. Engrg.
Ohio State University
Columbus, Ohio 43212.

References

[1] H. E. King, "Mutual impedance of unequal length antennas in echelon," *IRE Trans. Antennas and Propagation*, vol. AP-5, pp. 306–313, July 1957.
[2] L. Lewin, "Mutual impedance of wire aerials," *Wireless Engr.*, vol. 28, pp. 352–355, December 1951.
[3] S. A. Schelkunoff and H. T. Friis, *Antennas, Theory and Practice*. New York: Wiley, 1952, pp. 370, 401.
[4] H. C. Baker and A. H. LaGrone, "Digital computation of the mutual impedance between thin dipoles," *IEEE Trans. Antennas and Propagation*, vol. AP-10, pp. 172–178, March 1962.

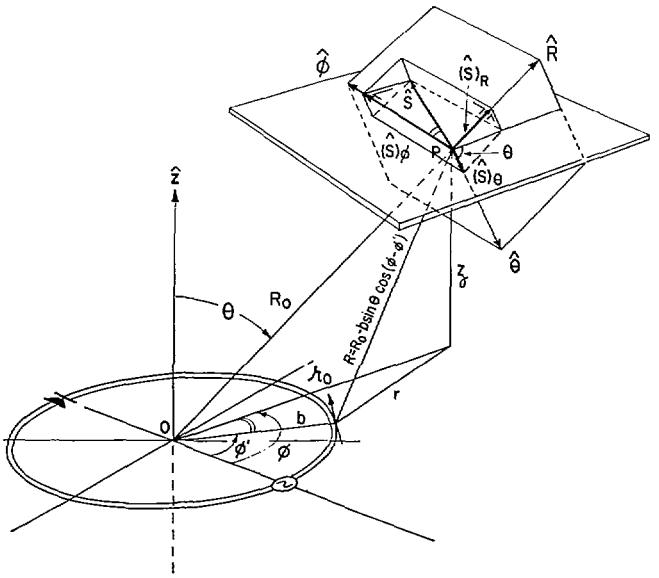

Fig. 1. Geometry of loaded circular loop.

Table of the Field Patterns of a Loaded Resonant Circular Loop

Abstract—**A table of *E*- and *H*-plane patterns of the circular loop antenna with $\beta b = 1.0$ loaded with $Z_L = R + jX$ at $\phi = 180°$ is presented. The table gives useful information for determining the values of the load impedance for a given field pattern. The results were experimentally examined.**

The purpose of this communication is to supply another table for the convenience of the antenna designer.

Theoretical investigations on loaded circular loops have been reported by relatively few authors [1]–[4] and very limited amounts of experimental data have been reported. This study is concerned with the systematic determination of the degree to which the radiation pattern of the loop can be altered by varying the load impedance. Experiments were performed to verify the more typical cases of the computations.

The loop with $\beta b = 2\pi/\lambda = 1$ was chosen because the current distribution along an unloaded loop of this size is in the dipole mode and is of particular interest [5]–[7]. It should be mentioned that, although the cases for the negative resistance are included, the prime purpose of the loading of such elements is not for amplification but rather for the alteration of the field pattern by significant changes in the current distribution along the loop caused by a negative resistance such as an Esaki diode.

The general expression for the far field of a thin wire at an observation point in terms of the unit vector R_0 and unit vector S along the wire that has an element of integration ds [8] is

$$E = \frac{j\omega\mu_0}{4\pi}\frac{1}{R_0}\int_s [\hat{R}_0 \times (\hat{R}_0 \times \hat{S})]I_s \exp(-j\beta R)\, ds \qquad (1)$$

where $\hat{R}_0$ is a unit vector pointing from 0 to P. With the aid of the geometry of the loaded circular loop in Fig. 1, (2) is obtained

$$E_\phi = \eta H_\theta = -\frac{j\omega\mu_0 b}{4\pi}\frac{\exp(-j\beta R_0)}{R_0} \cdot \int_0^{2\pi} I(\phi')\cos(\phi-\phi')\exp[j\beta b\sin\theta\cos(\phi-\phi')]\,d\phi'. \qquad (2)$$

Manuscript received October 24, 1969.

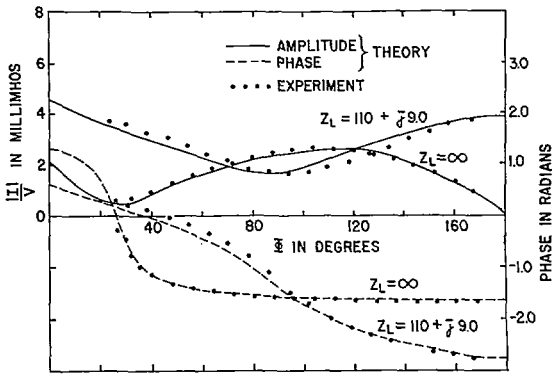

Fig. 2. Magnitude and phase distribution of current on loop with $\beta b = 1.0$ loaded with $Z_L = \infty$ at $\phi = 180°$ and with $Z_L = 110 = j9.0$ at $\phi = 180°$.

The radiation patterns can be obtained from (2) if the distribution of the current $I(\phi')$ for the loaded antenna is known. The expression for the current distribution $I(\phi')$ along such an antenna has been previously reported in [1, eq. (22)] without experimental verification. Experiments were conducted to verify (22) in our laboratory. The experimental results were found to be in agreement with the theory. A typical result is shown in Fig. 2.

The field patterns of the loaded loop with various values of load impedance Z_L can now be calculated using the experimentally verified expression for current. Fig. 3 shows the calculated patterns of the circular loop antenna with $\beta b = 1.0$ loaded with $Z_L = R + jX$. Because of symmetry, only one half of the entire pattern is shown. It also should be noted that both the E pattern $[E_\phi(\phi)$ with $\theta = 90°]$ and the H pattern $[E_\phi(\theta)$ with $\phi = 0$, $\phi = 180°]$ should meet at $\theta = 90°$, $\phi = 0°$, and $\theta = 90°$, $\phi = 180°$. The patterns with the same value of R are arranged in a column and those with the same value of X are placed in a row. The values of R and X used are -500, -150, -50, 0, 50, 150, and 500 ohms.

It is observed from the figure that, in general, larger changes in the radiation patterns take place in the columns; i.e., changes in X affect the radiation pattern more than do changes in R. However, for large changes in the radiation pattern, the values of both R and X have to be changed.

It is worthwhile noting that the position of the minimum of the E-pattern curves shifts toward larger values of ϕ as the value of R is